Palaeogeography, Palaeoclimatology, Palaeoecology 415 (2014) 48–58

Contents lists available at ScienceDirect

Palaeogeography, Palaeoclimatology, Palaeoecology

journal homepage: www.elsevier.com/locate/palaeo

Landscape evolution during the late Quaternary at the Doce River mouth, Espírito Santo State, Southeastern Brazil

Marcelo Cancela Lisboa Cohen [a,b,*], Marlon Carlos França [a], Dilce de Fátima Rossetti [c], Luiz Carlos Ruiz Pessenda [d], Paulo César Fonseca Giannini [e], Flávio L. Lorente [d], Antônio Álvaro Buso Junior [d], Darcilea Castro [c], Kita Macario [f]

[a] Laboratory of Coastal Dynamics, Graduate Program of Geology and Geochemistry, Institute of Geoscience, Federal University of Pará (UFPA), Rua Augusto Correa 01, 66075-110 Belém, PA, Brazil
[b] Oceanography Faculty, Federal University of Pará, Rua Augusto Corrêa, n 1, Guama, CEP: 66075-110, Belém, PA, Brazil
[c] National Institute for Space Research (INPE), Rua dos Astronautas 1758-CP 515, CEP: 12245-970 São José dos Campos, SP, Brazil
[d] Center for Nuclear Energy in Agriculture (CENA), 13400-000 Piracicaba, SP, Brazil
[e] Institute of Geoscience, Department of Sedimentary and Environment Geology, University of São Paulo, São Paulo, Brazil
[f] LAC-UFF AMS Laboratory, Fluminense Federal University, Physics Department, Niteroi, Rio de Janeiro, Brazil

ARTICLE INFO

Article history:
Received 31 May 2013
Received in revised form 13 November 2013
Accepted 4 December 2013
Available online 19 December 2013

Keywords:
Climate change
Isotopes
Palynology
Sea-level changes
Sedimentary facies

ABSTRACT

The sedimentary deposits of the deltaic plain of the Doce and Barra Seca rivers, Southeastern Brazil, were studied by facies analysis, pollen records, $\delta^{13}C$, C/N analysis and AMS ^{14}C-dating. Today, this deltaic plain is dominated by beach ridges and sandy terraces occupied by arboreal and herbaceous vegetation. Between ~47,500 and ~29,400 cal yr B.P., a deltaic system was developed in response mainly to eustatic sea-level fall. Although the studied stratigraphic succession is compatible with the trend of global sea-level fall, the earlier sea-level suggested by the topographic position of these deltaic deposits was above the one expected during the MIS3 stage. A tectonic uplift likely occurred during the late Quaternary and raised these deposits. The post-glacial sea-level rise caused a marine incursion with invasion of embayments and broad valleys, and it favored the evolution of an estuary with wide tidal mud flats occupied by mangroves between ~7400 and ~5100 cal yr B.P. The high river sand supply and/or the relative sea-level fall in the late Holocene led to seaward and downward translation of the shoreline during normal/forced regression, producing progradational deposits with shrinkage of mangrove stands and expansion of marshes colonized by herbaceous vegetation. Therefore, the stratigraphic architecture and evolution of the Doce River deltaic plain suggest that fluvial sediment supply and relative sea-level fluctuations related to Quaternary global climatic changes and local tectonism exerted major controls on sedimentation through the variation of accommodation space and base-level changes.

1. Introduction

Systematic studies of the Holocene sea-level in the eastern Brazilian coastline show a post-glacial sea-level rise and a middle Holocene sea-level highstand, with a subsequent fall to the present time (e.g., Angulo et al., 2006). Sea-level change and local sedimentary inflow are main factors controlling the evolution of sedimentary plains along the Brazilian coast. Several coastal environments occur along this coast, such as mangroves, beaches, lagoons, and deltas. These are environments that might compose an integrated system; thus they cannot be analyzed in isolation (Woodroffe, 2002).

The equilibrium profile of a sandy coastal zone is determined by local hydrodynamics and sediment grain sizes, which are controlled by tides, waves and littoral currents. However, a standard equilibrium profile will be established over a sufficiently long period of time. Although this equilibrium may be disturbed by relative sea-level rise (SLR), it would be re-established by a landward displacement of the beach profile. This process results in an accelerated erosion of the beach prism and transfer of eroded sands toward the inner shelf, producing a rise of the inner shelf bottom by a height equal to that of SLR (Bruun, 1962; Schwartz, 1965, 1968; Woodroffe, 2002).

The dominant depositional systems under rising sea-level on a gently sloping sandy coast are barrier islands or estuaries (Swift, 1975), while strandplains with beach-ridges are virtually absent. Regarding estuaries, their response to sea-level changes is affected by tidal range, nearshore wave climate and river inflow, as well as by the nature and supply of sediments. All estuaries assumed their present form during the rise of sea-level that followed the Last Glacial Maximum (LGM), about 20 thousand years ago (Chappell and Woodroffe, 1994). In contrast, a sea-level fall creates highly unfavorable conditions for the genesis and maintenance of estuaries, lagoons and bays, especially in wave

* Corresponding author at: Laboratory of Coastal Dynamics, Graduate Program of Geology and Geochemistry, Institute of Geoscience, Federal University of Pará (UFPA), Rua Augusto Correa 01, 66075-110 Belém, PA, Brazil. Tel./fax: +55 91 3274 3069.
E-mail address: mcohen@ufpa.br (M.C.L. Cohen).

0031-0182/$ – see front matter © 2013 Elsevier B.V. All rights reserved.
http://dx.doi.org/10.1016/j.palaeo.2013.12.001

dominated coasts. A continued river sediment supply results in shoreline progradation, and it may generate a delta (Suter, 1994). Under this condition, lagoons and bays become emergent and beach ridge plains rapidly prograde, resulting in regressive sand sheets (Martin and Suguio, 1992).

When present, mangroves along the littoral can be used as indicators of coastal dynamics, as their positions within the intertidal zone are strongly influenced by SLR (Woodroffe et al., 1989; Woodroffe, 1995). Over a range of SLR scenarios, coastal wetlands adjust toward an equilibrium with sea-level (e.g., D'Alpaos et al., 2007; Kirwan and Murray, 2007). Equilibrium models predict that coastal wetlands have a number of feedbacks that allow them to maintain their positions relative to the mean tidal range (Cohen et al., 2005a,b). For example, surface accretion, often through sediment inputs, increases with the depth of tidal inundation (e.g., French and Stoddart, 1992; Furukawa and Wolanski, 1996), leading to increments in surface elevation that allow the wetland to keep pace with sea-level rise (Cahoon et al., 2006). Fringe mangroves have kept up and could accommodate eustatic SLR rates of 4 mm/yr. If eustatic rates exceed 5 mm/yr, then the mangroves would not be likely to persist (Mckee et al., 2007).

The northern littoral of the Espírito Santo State features a deltaic plain associated with the Doce River. According to Martin and Suguio (1992), during the middle Holocene, almost all sediments supplied by the Doce River were retained within large lagoons located behind a barrier island. This was due to the Holocene relative sea-level highstand about 5.5 ky B.P. About 2.5 ky B.P., the coastal lagoons became completely filled. Today, this area is characterized by sand accumulation in vast strandplains, with mangroves being restricted to lagoon margins.

The aim of this study is to improve the reconstruction of landscape evolution in the Doce River delta plain, approaching the interaction among sedimentary processes, vegetation dynamics and sea-level fluctuations during the late Pleistocene and Holocene based on facies analysis, pollen records, $\delta^{13}C$, C/N analysis and AMS dating.

2. Study area

2.1. Location

The study site comprises the deltaic plain of the Doce River. Six sediment cores were sampled following a landward transect. These, named as Li in reference to the city of Linhares, which is located 30 km southwest of the study area, include: Li31 (S 19° 11′ 16″/W 39° 49′ 33″); Li01 (S 19° 10′ 53″/W 39° 51′ 55″); Li33 (S 19° 10′ 19.16″/W 39° 53′ 10″); Li26 (S 19° 07′ 4″/W 39° 52′ 57″); Li23 (S 19° 08′ 58″/W 39° 53′ 29″), and Li24 (S 19° 09′ 8″/W 39° 55′ 47″). Core Li24 was obtained at the margin of a paleochannel in the most proximal sector of the studied coastal plain (Fig. 1c), whereas core Li31 was taken from a lake confined between beach ridges. Cores Li23, 26 and 33 were from the coastal plain dominated by beach ridges, and core Li01 (located 10 km from Li24) was collected at the margin of Lake Bonita, which is a freshwater lake in the lower course of the Barra Seca River (Fig. 1c) in the Sooretama Federal Biological Reserve. This lake is 30 km from the Doce River and 15 km from the sea in this wave-dominated coast of Brazil (Dominguez, 2009).

2.2. Geology and geomorphology

Four geomorphological units are recognized in the area: (1) a mountainous area, represented by Precambrian crystalline rocks, with a multidirectional rectangular dendritic drainage net; (2) a tableland area composed of the Barreiras Formation, which consists of sandstones, conglomerates, and mudstones attributed mainly to Neogene fluvial and alluvial fan deposits, but possibly including marine deposits originated from a coastal onlap associated with Neogene transgressions (Arai, 2006; Dominguez, 2009); (3) a coastal plain area, with fluvial, transitional and shallow marine sediments deposited during changes in sea-level in the Quaternary (Martin and Suguio, 1992); and (4) an inner continental shelf area (Asmus et al., 1971). Several W–E, NW–SE and NE–SW tectonic lineaments reveal the importance of regional tectonics in the development of many of the modern drainage systems (Fig. 1a).

Currently, the Doce River shows a mostly W–E trending "straight" pattern, flowing on basement crystalline rocks and into the littoral plain through a low valley with Holocene terraces (Fig. 1a). The terraces, with a 0.45% longitudinal gradient, consist of a mixture of sediments from the Barreiras Formation that were transported by rivers that originated in mountainous areas and Neogene tablelands. The deposits are composed mainly of moderately sorted, coarse- to very-coarse grained sands of beach ridges distributed along the coastline. Downstream, sandy silts of the Doce River spread over floodplains (Fig. 1a). Residual and very poorly preserved mangrove vegetation close to marine influence occurs at the margin of coastal lagoon system. An elongated coastal sand barrier occurs parallel to the shore and is separated from the mainland by a lagoon. It is 37 and 3.6 km in length and width, respectively, and has multiple beach ridges that likely represent successive shoreline positions formed during coastline progradation associated with sea-level fall (Otvos, 2000).

The studied delta plain covers an area of ~2700 km^2. It displays fluvial channels and an extensive paleochannel network. The abandoned channels are straight to meandering, and they maintain the shape and typical concavity of the original channel, resulting in the formation of lakes and lake belts (Fig. 1c). Avulsion may have been responsible for the partial or complete abandonment of several channels due to rapid sand accumulation.

The sandy ridges are extensive, straight to slightly curved sand bodies colonized by herbaceous vegetation, and they exhibit N–S and NW–SE orientations, elevations between 4 and 11 m, lengths of 2 to 20 km, and interridge spacings between 30 and 200 m (Fig. 1b). Additionally, the studied delta plain has three topographic groups of sandy ridges, named inner (~9 m), intermediated (~5 m) and outer sandy ridge (~10 m) with maximal widths of about 3.5, 75 and 3.6 km, respectively. The inner and intermediate sandy ridges are interpreted as beach ridges, whereas the outer sandy ridges occur as dune ridges. Some interridge depressions contain standing water. These shallow interridge lakes are subjected to overbank crevassing, resulting in a sediment influx into the lakes. They are ~2 m in depth, ephemeral and have water salinity of ~0‰, which are characteristics due to the seasonality of climate and hydrology. The deposits consist of thick peat layers, laminated mud and bioturbated mud, and are colonized by freshwater marshes.

2.3. Climate

The region is characterized by a warm and humid tropical climate with annual precipitation averaging 1400 mm (Peixoto and Gentry, 1990), which is concentrated in the summer, between November and January. The dry fall–winter season occurs between May and September. It is regulated by the position of the Inter Tropical Convergence Zone (ITCZ) and the South Atlantic Convergence Zone (SACZ) (Carvalho et al., 2004). The study area is entirely located within the South Atlantic trade wind belt (NE–E–SE) that is related to a local high-pressure cell and the periodic advance of the Atlantic Polar Front during the autumn and winter, which generates SSE winds (Dominguez et al., 1992; Martin et al., 1998). The average temperature ranges between 20 °C and 26 °C.

2.4. Vegetation

The modern vegetation is composed mainly of tropical rainforest. The most representative plant families are Fabaceae, Myrtaceae, Sapotaceae, Bignoniaceae, Lauraceae, Hippocrateaceae, Euphorbiaceae, Annonaceae and Apocynaceae (Peixoto and Gentry, 1990). An herbaceous plain mainly represented by Cyperaceae and Poaceae with some

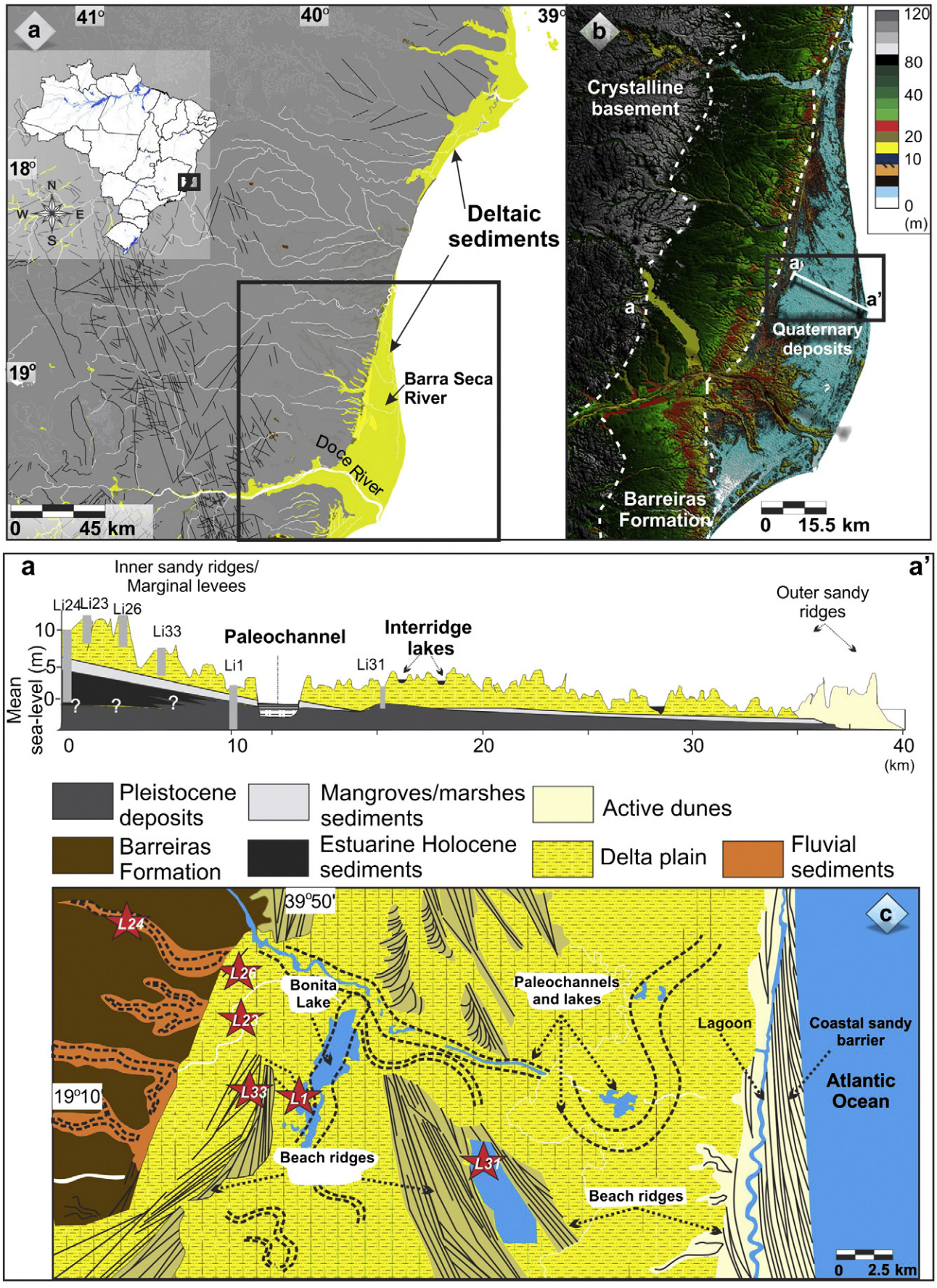

Fig. 1. a) Location of the study area and its geological context. b) SRTM-DEM topography of the study site and lithostratigraphic profiles. c) Location of studied sediment cores and the spatial distribution of main geomorphological features.

trees and shrubs occurs on the edges of the proximal portion of the delta plain. A gradual transition occurs toward the distal portion of the delta plain close to the shoreline, which is dominated by *restinga* vegetation over sand plains and dunes. This consists of shrubs and herbs. Palm trees, as well as orchids and bromeliads growing on trunks and branches of larger trees, are also present along the shoreline. These associated with *Ipomoea pes-caprae* (Convolvulaceae), *Hancornia speciosa* (Apocynaceae), *Chrysobalanus icaco* (Chrysobalanaceae), *Hirtella Americana* (Chrysobalanaceae), *Cereus fernambucensis* (Cactaceae), *Anacardium occidentale* (Anacardiaceae) and *Byrsonima crassifolia* (Malpighiaceae). Mangroves represented by *Rhizophora* and *Avicennia* are restricted to the margin of the lagoons. The vegetation inside the Lake Bonita and at its margins comprises *Tabebuia cassinoides*, *Alchornea triplinervia* and *Cecropia* sp., and emersed, submerged, floating-leaved and floating plants like *Typha* sp., Cyperaceae, Poaceae, *Salvinia* sp., *Cabomba* sp., *Utricularia* sp. and *Tonina* sp. A freshwater marsh composed by herbaceous vegetation colonizes the Barra Seca Valley.

3. Methods

3.1. Remote sensing

The morphological aspects of the study area were characterized based on analysis of the Landsat 5-TM images that were obtained in August 2008 by the Brazilian National Institute for Space Research (INPE). The digital elevation model (DEM) derived from the Shuttle Radar Topographic Mission (SRTM-90 m) and distributed by the National Aeronautics and Space Administration (NASA) was additionally used in this study. The SRTM-DEM data were processed using customized shading schemes and palettes to highlight the topographic and morphological features. We interpreted elevation data using the software Global Mapper (Global Mapper Software LLC, Olathe, KS, USA).

3.2. Sampling processing and facies description

A fieldwork campaign was undertaken during the dry season of November 2009. Using a Percussion Drilling (Hammer Cobra TT), sediment cores were taken to a depth of as much as 12 m. Following the proposal of Harper (1984) and Walker (1992), facies analysis included descriptions of lithology, texture and structures. The sedimentary facies were codified following Miall (1978). The sediment grain size distribution, following Wentworth (1922), was analyzed by laser diffraction in a Laser Particle Size SHIMADZU SALD 3101.

3.3. Pollen and spore analysis

For pollen analyses, 1 cm^3 samples were taken at 10 cm intervals along cores Li01 and Li24. Preparation followed standard pollen analytical techniques including acetolysis (Faegri and Iversen, 1989). Pollen and spores were identified by comparison with reference collections of about 4000 Brazilian forest taxa and various pollen keys (Salgado-Laboriau, 1973; Absy, 1975; Markgraf and D'Antoni, 1978; Roubik and Moreno, 1991; Colinvaux et al., 1999), jointly with the reference collection of the Laboratory of Coastal Dynamics of the Federal University of Pará, and of the ^{14}C Laboratory of the Center for Nuclear Energy in Agriculture (CENA/USP). A minimum of 300 pollen grains were counted for each sample, except at specific depths where only 100–200 grains were counted due to low pollen concentration. Microfossils consisting of spores, algae and fungi were also counted but not included in the sum. Pollen data are presented in pollen diagrams as percentages of the total pollen sum. Taxa were grouped into broad ecological categories including mangrove, trees and shrubs, herbs, palms, fern spores, and micro-foraminifer. The software TILIA was used for calculations, and the CONISS and TILIAGRAPH softwares for both the cluster analysis of pollen taxa and the plot of the pollen diagrams (Grimm, 1987).

3.4. Isotopic and chemical analysis

Ninety-four samples (1 cm^3) were collected along cores Li01 and Li24. Samples were separated and treated with 4% HCl to eliminate carbonates, washed with distilled water until at pH ~ 6, dried at 50 °C, and homogenized. These samples were used for analyses of total organic carbon (TOC) and total nitrogen (TN) concentrations and carbon stable isotopic compositions that were carried out at the Stable Isotope Laboratory of the Center for Nuclear Energy in Agriculture (CENA/USP). The concentration results are expressed in percent of dry weight after the removal of carbonate, with an analytical precision of 0.09 and 0.07%, respectively. The C/N values represent the molar ratio between carbon and nitrogen. The ^{13}C results are expressed as $\delta^{13}C$ with respect to the VPDB standard using the following conventional notations:

$$\delta^{13}C(‰) = \left[\left(R_{1sample}/R_{2standard}\right) - 1\right] \cdot 1000$$

where RS_1 and RS_2 are, respectively, the $^{13}C/^{12}C$ ratios in the sample, RPDB the $^{13}C/^{12}C$ ratio for the international standard (VPDB). The results are expressed in delta per mil (δ ‰) notation, with analytical precision better than 0.2‰ (Pessenda et al., 2004).

3.5. Radiocarbon dating and sedimentation rates

Thirteen samples of ~2 g each of sedimentary organic matter and one shell were used for radiocarbon dating (Table 1). The sediment samples were physically treated by removing roots and vegetation fragments under the microscope. The residual material was then treated with 2% HCl at 60 °C for 4 h, and then washed with distilled water until neutral pH and dried (50 °C) to remove probable younger organic fractions (fulvic/humic acids) and carbonates. The chronologic framework was provided by accelerator mass spectrometer (AMS) radiocarbon dating. Samples were analyzed at the ^{14}C Laboratory of Fluminense Federal University (LACUFF) and at the University of Georgia – Center for Applied Isotope Studies (UGAMS). Radiocarbon ages were normalized to a $\delta^{13}C$ of −25‰ VPDB and reported as calibrated years (cal yr B.P.) (2σ) using CALIB 6.0 (Reimer et al., 2009). The dates are reported in the text as the median of the range of calibrated ages. Sedimentation rates were based on the ratio between the mean depth intervals (mm) and the mean time range.

4. Results

4.1. Radiocarbon dates and sedimentation rates

The dating results revealed ages ranging from 49,391–45,775 cal yr B.P. to recent. The filling of the estuary, as represented in core Li24, is recorded by an upward decrease of sedimentation rates from 9.4 mm/yr (9.5–6.7 m), 8.1 mm/yr (6.7–5 m), 0.5 mm/yr (5–3 m) to ~1.4 mm/yr (3–1 m). A partial age overlapping was identified in core Li01 between 6.2 and 8.8 m. This overlap can probably be attributed to the type of dated material, because a shell and sedimentary organic matter were dated at 6.20–6.30 and 8.8–8.86 m depths, respectively (Fig. 3). Generally, the organic matter found in marine sediments is suitable for radiocarbon dating, assuming a true temporal relation between the material dated and the timing of sedimentation. However, it is possible that overgrowth of calcite in mollusc and gastropods shells incorporated old carbon from limestone or calcareous sediments, consequently yielding radiocarbon ages that are ~3000 ^{14}C years older (Rubin et al., 1963; Evin et al., 1980; Goodfriend and Stipp, 1983; Goodfriend, 1987; Pigati et al., 2013). Core Li31 had an age inversion between 1.10 and 5 m (Figs. 2 and 3) that was recorded at the base and top of the fluvial channel facies association. This inversion may reflect a rapid filling of the channel and/or reworking of older sedimentary organic matter (Fig. 2).

Table 1
Radiocarbon dates of studied sediment cores.

Lab. number	Sample	Depth (m)	Dated material	Ages (^{14}C yr BP, 1σ)	Ages (cal yr BP, 2σ)	Mean (cal yr BP, 2σ)
UGAMS 10565	LI 1	1.65–1.75	Sed. org. matter	6710 ± 30	7556–7622	~7600
UGAMS 10566	LI 1	3.7–3.75	Sed. org. matter	24,610 ± 70	29,226–29,678	~29,500
LACUFF13018	LI 1	6,20–6,30	Shell	33,358 ± 948	36,105–40,014	~38,000
UGAMS11693	LI 1	8.80–8.86	Sed. org. matter	31,220 ± 100	35,162–36,321	~35,700
LACUFF00038	LI 1	11.52–11.7	Sed. org. matter	44,232 ± 812	45,775–49,391	~47,500
UGAMS 10567	LI 24	1	Sed. org. matter	Modern	Modern	Modern
UGAMS 10568	LI24	3	Sed. org. matter	1480 ± 25	1313–1405	~1350
UGAMS 10569	LI 24	5	Sed. org. matter	4500 ± 25	5047–5201	~5100
UGAMS 10570	LI 24	6.7	Sed. org. matter	6330 ± 30	7171–7317	~7200
UGAMS 10571	LI 24	9.5	Sed. org. matter	6560 ± 30	7425–7509	~7500
UGAMS 10572	LI 31	1.05–1.1	Sed. org. matter	4320 ± 25	4840–4893	~4860
UGAMS 10573	LI 31	4.95–5.0	Sed. org. matter	3600 ± 20	3845–3933	~3890
UGAMS 10574	LI 31	6.55–6.65	Sed. org. matter	25,970 ± 80	30,465–31,022	~30,700

4.2. Facies description

The studied cores record sedimentary successions encompassing massive sand and mud, parallel laminated/cross stratified sand and wavy/lenticular heterolithic deposits (Fig. 2). Pollen, spore, shell records and $\delta^{13}C$ values were added to facies characteristics in order to define nine facies associations.

4.2.1. Deltaic and central estuarine basin/lagoon (A)

The deltaic deposits consist of five facies associations related to high and low energy proximal environments of the deltaic system. The sedimentary deposits of the estuary central basin/lagoon occur only in the base of core Li24.

4.2.1.1. Facies association A1—Beach ridge complex. This facies association occurs in core Li01 between 0 and 1.8 m depth; core Li23 between 0 and 2.2 m; core Li26 between 0 and 5 m, and throughout core Li33. It is characterized by silty to fine-grained sands and laminated muds with plant remains that grade upward into coarse-grained sandy deposits with cross-laminated or cross-stratified sand, characterizing coarsening upward successions. In core Li33, it consists only of cross-laminated and cross-stratified sands. Association A1 ranges in thickness from a few cm up to 2 m thick (Fig. 2).

A pollen assemblage that was identified mainly in the finer-grained layers of core Li01 is predominantly characterized by herbs (30–100%) represented by Poaceae (30–60%), Cyperaceae (9–40%) and Asteraceae (0–7%) and by trees and shrubs, evidenced mainly by Fabaceae (0–50%) and Sapotaceae (0–17%).

4.2.1.2. Facies association A2—Lake. This facies association occurs only in core Li31 between 0 and 1.2 m in the upper part of facies association A3.

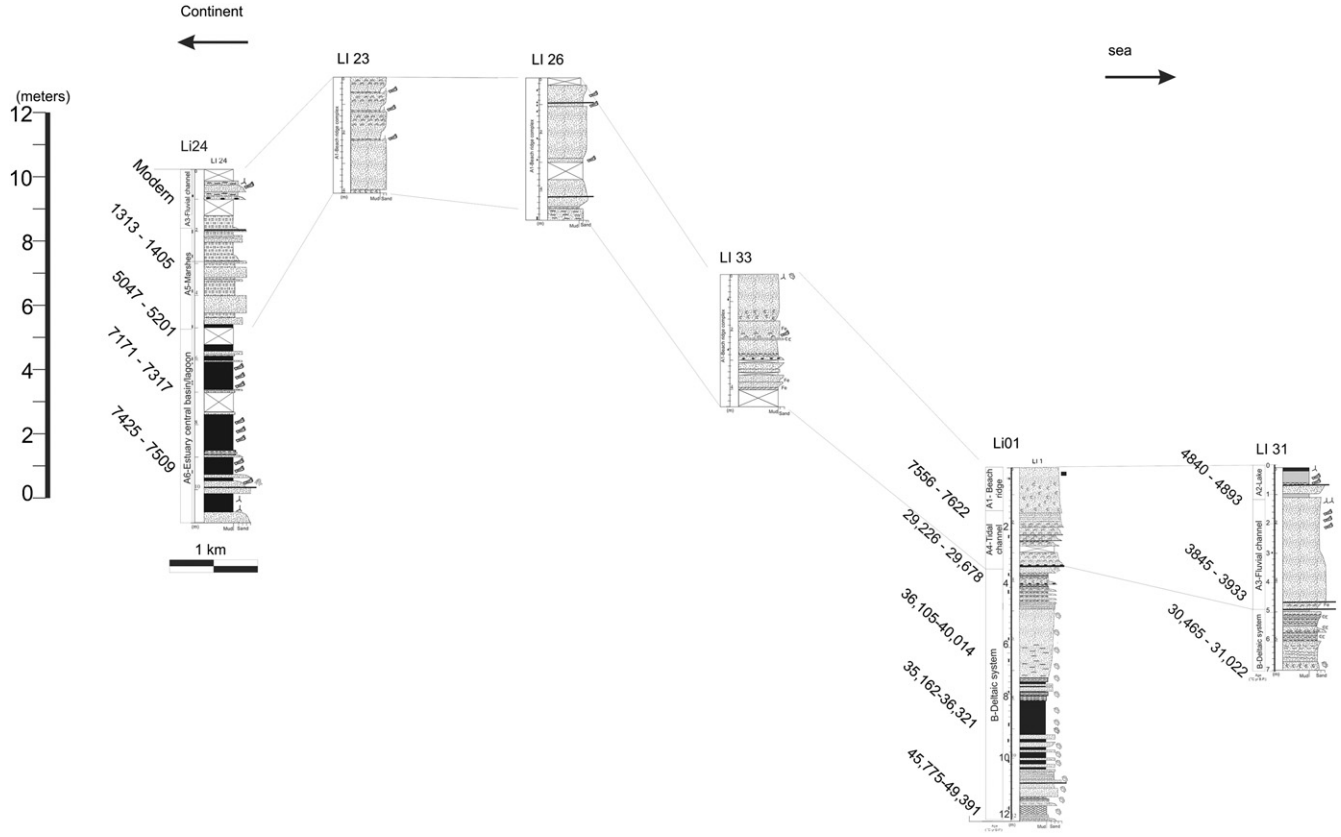

Fig. 2. Topographic correlation among the facies associations identified in the studied cores.

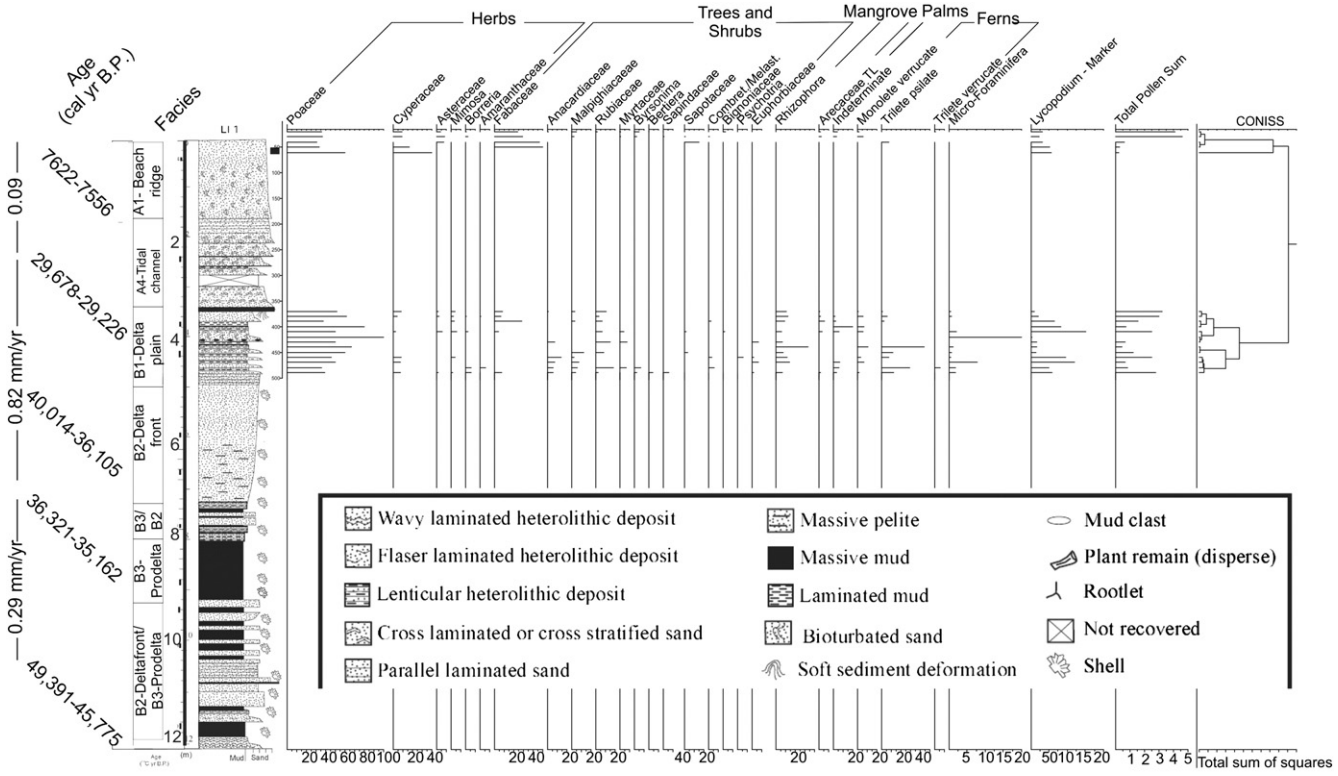

Fig. 3. Stratigraphic description for core Li01 with lithological profile, pollen analysis and geochemical variables.

It is characterized by massive mud with plant remains that become interbedded with sand layers in its base.

4.2.1.3. Facies association A3—Fluvial channel. This association occurs in cores Li24 (0–1.8 m) and Li31 (1.2–4.6 m). It consists of several thin fining upward successions of massive, cross-stratified or cross-laminated, fine- to coarse-grained sands in core Li24 and massive medium to coarse-grained sands in core Li31. These deposits are typically bounded at the base by sharp erosional surfaces, which are sometimes mantled by a lag of quartz granules or mud clasts. The pollen assemblage in the finer-grained layers in core Li24 presents arboreal (70–86%) pollen as being the most representative, followed by herbaceous (10–15%) pollen (Fig. 4). The $\delta^{13}C$ values range between −28‰ and −26‰. The C/N values are between 6 and 12 (Figs. 4 and 5).

4.2.1.4. Facies association A4—Tidal channel. This association is represented in core Li01 (1.6–2.6 m). It consists of several thin fining upward successions of massive, cross-stratified or cross-laminated, fine- to coarse-grained sands (Fig. 3). This facies association is characterized by $\delta^{13}C$ values between −28‰ and −24‰, and C/N values between 7 and 46 (Fig. 5).

4.2.1.5. Facies association A5—Marshes. This association occurs in core Li24, between 1.8 and 5 m depth, and consists of organic mud (peat

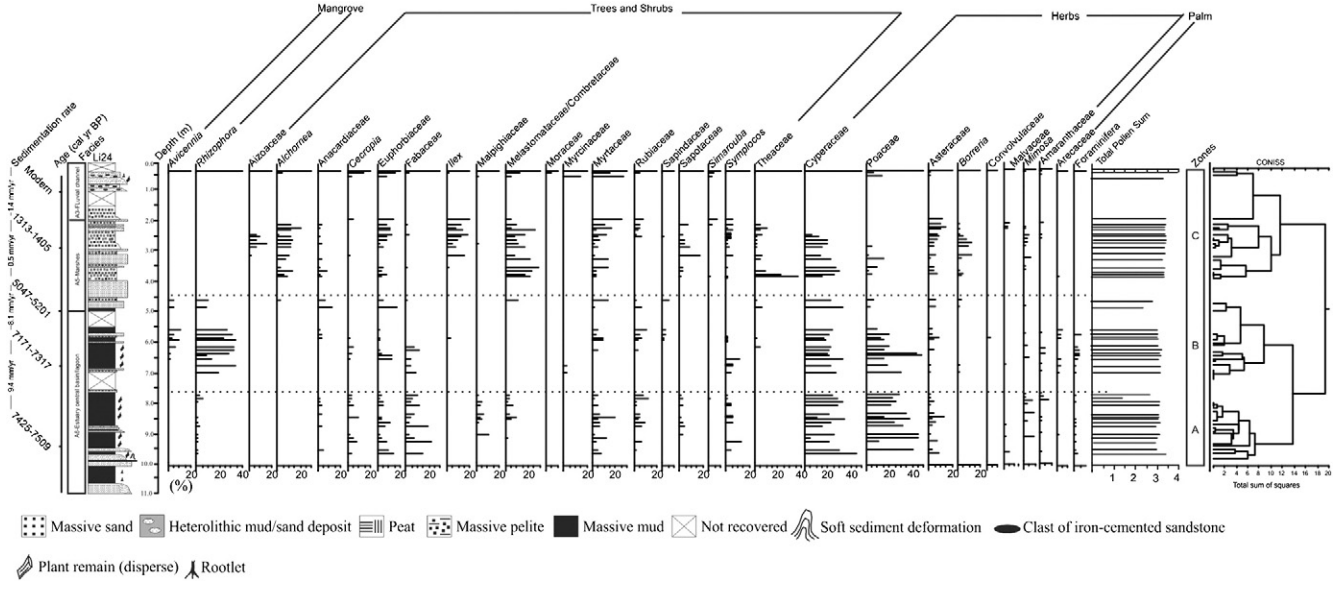

Fig. 4. Stratigraphic description for core Li24 with lithological profile, pollen analysis and geochemical variables.

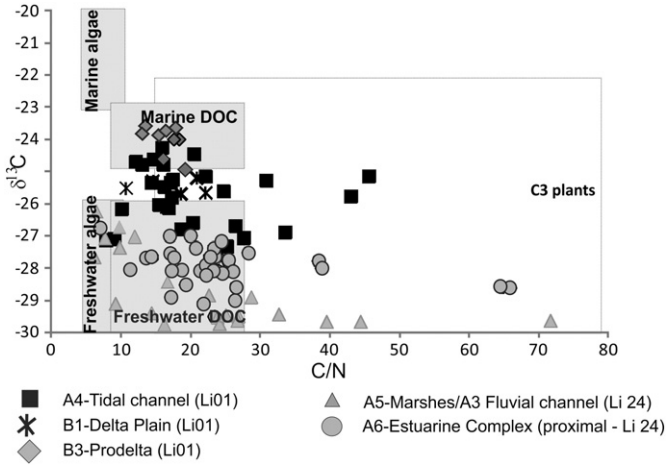

Fig. 5. Diagram illustrating the relationship between $\delta^{13}C$ and C/N (molar ratio) for the different sedimentary facies, with interpretation according to data presented by Lamb et al. (2006) and Meyers (2003).

layer) interbedded with sand. These deposits contain arboreal pollen (60–85%), mainly represented by Melastomataceae/Combretaceae (0–30%), *Alchornea* (0–20%), Myrtaceae (0–25%), Euphorbiaceae (0–15%), *Ilex* (0–20%) and Sapotaceae (0–20%), followed by herbs pollen (20–60%) composed by Cyperaceae (1–30%), Poaceae (0–15%), *Borreria* (0–15%), Aizoaceae (0–20%), Asteraceae (0–15%) and *Mimosa* (0–5%) (Fig. 4). The $\delta^{13}C$ values range between −26‰ and −30‰, and the C/N values occur between 9 and 71 (Fig. 5).

4.2.1.6. Facies association A6—central estuarine basin/lagoon. This facies association was recorded in core Li24 between 4.5 and 11 m, and it is represented by massive mud with plant remains interbedded with sand deposited during the early Holocene. This phase is characterized by arboreal and herbaceous pollen (Fig. 4). These deposits are dominantly muddy. The sedimentary facies grades upward into tidal flat colonized by mangroves with thickening and coarsening upward successions. Trees and shrubs (20–45%) and herbs (35–73%) pollen, followed by mangrove (15–43%) pollen represented by *Rhizophora* (10–30%) and *Avicennia* (5–10%) are preserved, occurring between 4.5 and 7 m in a massive mud with sand. Between 7 and 11 m occur trees and shrubs (20–60%) and herbaceous (40–75) pollen (Fig. 4). This facies association is characterized by $\delta^{13}C$ values between −29 and −27‰. The C/N values display a range of variation between 8 and 66 (Fig. 5).

4.2.2. Deltaic system (B)

This depositional system is recorded between 5 and 7 m in core Li31 (Fig. 2) and between 3.4 and 12 m depth in core Li01 (Fig. 3). It is represented by three facies associations: B1—Delta Plain, B2—Deltafront, and B3—Prodelta.

4.2.2.1. Facies association B1—Delta Plain. This association is mainly characterized by gray massive and laminated mud with massive sandy levels between 7 and 5 m in core Li31 (Fig. 2), and between 3.6 and 5.0 m in core Li01 (Fig. 3). The pollen assemblages in this interval in core Li01 are characterized by the predominance of herb pollen (35–96%) represented by Poaceae (36–96%), Cyperaceae (0–8%), Asteraceae (0–5%), *Mimosa* (0–5%), *Borreria* (0–5%) and Amaranthaceae (0–5%). The pollens of trees and shrubs are represented mainly by Fabaceae (0–28%), Anacardiaceae (0–14%), Malpighiaceae (0–12%), *Byrsonima* (0–5%), Rubiaceae (0–18%) and Myrtaceae (0–5%). The mangrove is characterized by *Rhizophora* (5–32%). Arecaceae, and ferns occurred also during this phase (Fig. 3). This facies association has $\delta^{13}C$ values between −26 and −25‰. The C/N values display a range of variation between 11 and 23 (Fig. 5).

4.2.2.2. Facies association B2—Delta Front. This facies association was record in the 5–8 m and 9.2–12 m intervals in core Li01 (Fig. 3). Between 5 and 7.5 m, it consists of a dark silt to medium-grained quartz sand, and it contains shells (*Olivella mutica*, *Glycymeris* sp., *Halistylus columna*, *Corbula cymellain*, *Mulinia cleryana*, *Tivela* sp., *Strigilla mirabilis* and *Miltha childrenae*) that may be scattered within the sediment or concentrated in layers. These species are found in sandy–muddy sediments from coastal areas near the mouths of rivers or oceanic islands (Da Costa, 1778; Say, 1822; Dall, 1881, 1890). The *Mulinia cleryana* may be found in coastal regions at depths between 0 and 30 m (Orbigny, 1846). The *Tivela* sp. occurs in water between 0 and 20 m (Link, 1807). *Olivella mutica* is found at depths to 113 m (Say, 1822). The *Halistylus columna* occurs between 18 and 108 m (Dall, 1890), while the *Strigilla mirabilis* and *Miltha childrenae* may be found between 10 and 65 m depth (Gray, 1825; Orbigny, 1841; Philippi, 1841).

The 7.5–8 m and 9.2–12 m intervals present characteristics of deltafront and prodelta settings with massive sand and dark clay levels. These intervals contain shells (*Anachis isabellei*, *Natica* sp., *Olivella floralia*, *Anadara ovalis*) scattered in the sediment. These species are found in sandy–muddy sediments from coastal areas near the mouths of rivers or oceanic islands (Bruguière, 1789; Duclos, 1840; Orbigny, 1841), whereas the *Anadara ovalis* may be found in coastal waters associated with carbonate and coral reefs (Bruguière, 1789).

4.2.2.3. Facies association B3—Prodelta. This facies occurs between 8 and 9.2 m and is represented by massive dark clay. Shells are present along this interval, but due to their poor preservation, we could not identify them. This facies association is characterized by $\delta^{13}C$ values between −25 and −23‰. The C/N values display a fairly narrow range of variation between 13 and 19 (Fig. 5).

5. Palaeoenvironmental interpretation

The base of core Li01 (12–9.2 m) likely represents sediment from a transition zone between delta front and prodelta that accumulated between ~47,500 and ~35,000 cal yr B.P., whereas the upward successions deposited in 9.2–8 m and 8–7.5 m intervals accumulated in a prodelta and prodelta/delta front environments, respectively (Fig. 6). The prodelta is entirely subaqueous and presents the finest-grained portion of a delta. Sediments here are deposited mostly from suspension or from dilute turbidity current flows. The finest sediments are found at the greatest depths, and usually a coarsening-upward signature is present. Relatively slow or intermittent deposition can permit marine organisms to colonize the sediments of the prodelta (Suter, 1994).

The sediments that accumulated between 7.5 and 5 m probably record a delta front that is the transition zone from the fluvial to the marine environment. The delta front includes distal bar silts, distributary mouth bar sands, and redistributed marine deposits such as tidal ridges and shoreface deposits. The process of river mouth sedimentation and seaward fining of sediments results in the deposition of the coarsest material a short distance from the river mouth on the upper parts of the delta front (Suter, 1994). The sedimentary deposits between 5 m and 3.6 m should represent a deltaic plain with its tidal flats, lagoons, mangroves and creeks (Suter, 1994; Figs. 3 and 6). The deltaic sediments that accumulated between ~47,500 and ~29,000 have $\delta^{13}C$ values ranging between −26‰ and −23‰, and C/N values between 11 and 23 (Fig. 5), indicating a mixed continental organic matter (C3 plants) and freshwater/marine algae influence (−30‰ to −26‰ and −23‰ to −16‰, respectively, Schidlowski et al., 1983; Meyers, 1994).

Facies association A6 (Estuary central basin/lagoon–bay) that accumulated during the early and middle Holocene (Fig. 4)represents low flow energy, likely in a depositional environment characterized by shallower water protected from direct wave action. However, this paleosetting is subject to some currents, as indicated by the presence of lenticular heterolithic mud deposits with sand levels and locally cross laminated sand. The C/N values between 8 and 66 and $\delta^{13}C$ values

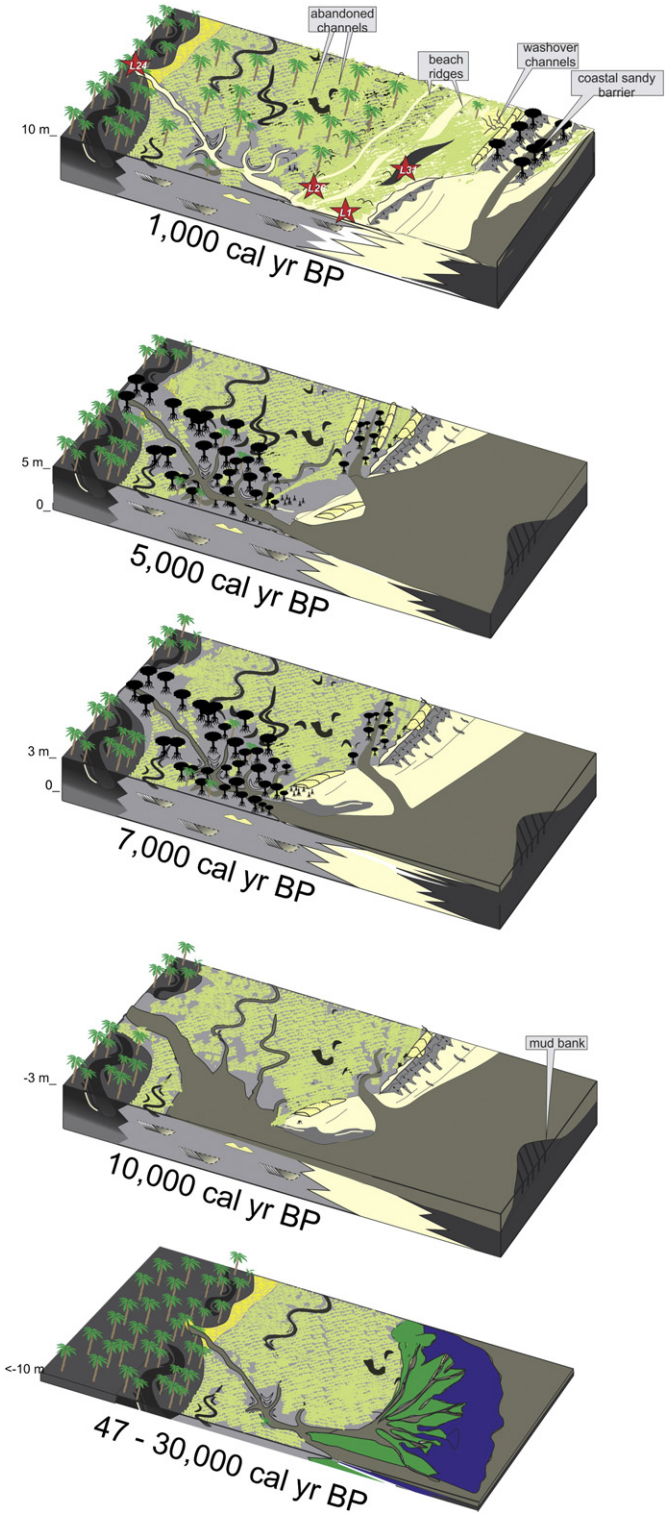

Fig. 6. Schematic representation of successive phases of sediment accumulation and vegetation change in the study area according to relative sea-level changes and sediment supply. (⋆ core locations).

ranging between −29‰ and −27‰ (Fig. 5) indicate varying continental organic matter (C3 plants) and freshwater algae influence (Fig. 5) (Schidlowski et al., 1983; Meyers, 1994), revealing a proximal portion that developed in an estuary, and in particular in the central portion of the estuary where the low-energy situation occurs (Fig. 6). Within an estuary, sediment is coarsest within the marine- and river-dominated zones and finest in the central zone (Dalrymple et al., 1992). However, the formation of barrier islands during the early Holocene may have contributed to the deposition of this sedimentary deposit, as described by Martin et al. (2003) and França et al. (2013). Therefore, the facies association A6 may have been deposited in an estuarine central basin or in a lagoon influenced by a river with its edge colonized by mangroves and herbaceous vegetation merging upward into marshes of the association A4 (Figs. 3 and 6).

Today, some mangroves occur immediately behind the coastal sandy barriers, which favors the lagoon development. As its tidal inlets experience longshore migration, the inlet channel is often obliterated as the sands from the adjacent barriers migrate.

The facies associations A1, A2, A3 and A5 are compatible with a deltaic plain setting, given that the study area today contains several sandy ridge sequences and has fluvial channels, lake belts and an extensive paleochannel network (Fig. 1).

The association A4 in core Li01 (Fig. 3) may correspond to a tidal channel established during the early Holocene and therefore represents a distal portion of the estuarine complex that was relatively more influenced by marine organic matter, as evidenced by the relation of the $\delta^{13}C$ and C/N values (Figs. 5 and 6). The sandy deposits occur in tidal channels that run the length of the estuary (Woodroffe et al., 1989; Dalrymple et al., 1990). Nevertheless, an energy minimum is recorded in the location of the finest channel sands. Muddy sediments accumulate primarily in tidal flats and marshes along the sides of the estuary. The appearance of these sediments in facies association A4 is related to marshes (A5) and the estuarine central basin/lagoon (A6).

The succession A3–A2 in core Li31 likely evidences abandonment phases of a channel by avulsion during the middle Holocene. The concavity of the some abandoned channels, products of the avulsion process, may result in formation of lakes (Figs. 1 and 2).

Facies association A1 is related to a beach ridge complex based on the sandy coarsening upward nature and on the relation with the other coastal associations. The wave-deposited sections run parallel to a shoreline, and, generally, as relative sea-level falls, the interridge depressions form shallow lakes subject to overbank crevassing, resulting in an influx of sediment into the lake ending with its siltation as identified in facies association A1 (Fig. 2, Li23).

Facies association A has $\delta^{13}C$ values predominantly around −28‰ (core Li24, Fig. 5) and −26‰ (core Li01, Fig. 5). The C/N values oscillate between 6 and 72 in core Li24, whereas in core Li01 the values are between 10 and 45. These values indicate contributions of C3 plants in facies association A3 and A4, as evidenced also by the pollen analysis (Fig. 5).

6. Climate and sea-level changes during the late Quaternary

Climate during Marine Isotope Stage 3 (MIS3), the phase that preceded the LGM, was globally 2 °C warmer than in the LGM (van Meerbeeck et al., 2009). Considering the South America, paleoecological studies indicate that the climate was 4–5 °C colder than the modern one during MIS3 (Stute et al., 1995; Behling, 1996, 2001; Behling et al., 1999; Colinvaux et al., 2000; Ledru et al., 2001; Burbridge et al., 2004; Urrego et al., 2005; Whitney et al., 2011). During the LGM in South America, temperatures were between 5 and 9 °C colder than present (Stute et al., 1995; Behling, 1996; Colinvaux et al., 1996; Haberle and Maslin, 1999; Mayle et al., 2000; Ledru et al., 2001; Bush et al., 2004). The onset of the LGM is defined as the time when sea-levels first approached their minimum levels at about 30 ky cal B.P. (Lambeck et al., 2002). Based on this interpretation, sea-levels suggest a duration of 10,000 yr for the LGM (between 30 and 19 ky cal B.P.). However, Peltier and Fairbanks (2006) suggest that the LGM must have started 26 ky cal B.P., having duration of about 5000–7000 years (between 26 and 19 ky cal B.P.).

During that time, the North Atlantic temperature was cooled by 8 °C or more and sea ice was more extensive than it is today (e.g. Ruddiman, 2008). Changes in sea-level are directly related to changes in global ice volume, where with each 1-m rise of sea-level equivalent to 0.4 million km^3 of ice (Ruddiman, 2008). According to global sea-level data based on independent proxies and modeled reconstructions (Imbrie et al., 1984; Chappell and Shackleton, 1986; Labeyrie et al., 1989; Bassinot et al., 1994; Lambeck, 1997; Rohling et al., 1998; Skene et al., 1998; Toscano and Lundberg, 1999; Shackleton, 2000; Lambeck and Chappell, 2001; Waelbroeck et al., 2002; Cutler et al., 2003; Siddall et al., 2003; Rubineau et al., 2006), global sea-level at 50 ky cal B.P. was between 40 and 80 m below the present, and sea-level fell gradually until 30–25 ky cal B.P., when it dropped abruptly (100–140 m below the modern sea-level) until ~20 ky cal B.P. After the end of the LGM, global sea-level rose dramatically (Fairbanks, 1989; Bard et al., 1990, 1996; Lambeck and Bard, 2000; Lambeck et al., 2002, 2004a,b; Berné et al., 2007; Clark et al., 2009; Bard et al., 2010). Based on geomorphic indicators, a similar trend was recorded along the continental shelf of the State of Rio de Janeiro (Reis et al., 2013).

In the present work, the observed succession of facies associations B and A might be a product of driving forces regulated by cyclic mechanism leading to a delta, estuary and leading to a deltaic plain environment. The changes in this depositional environment were probably driven by the equilibrium between relative sea-level changes and fluvial sediment supply during the late Pleistocene and Holocene. The depositional architecture of the Late Pleistocene coastal system probably evolved from a prodelta to a delta front, followed by the deltaic plain in response to relative sea-level fall between ~47,500 and ~29,400 cal yr B.P. (Fig. 6).

Sediments that accumulated during the LGM and the Late Pleistocene/Holocene transition were not identified. Probably from ~29,400 cal yr B.P. to ~7500 cal yr B.P in core Li01, and ~30,000 cal yr B.P. to ~3900 cal yr B.P. in core Li31, a sedimentary hiatus occurred that was related to erosion associated with the rapid post glacial sea-level rise. A similar erosive event between ~19,000 cal yr B.P. and ~2200 cal yr B.P. has been recorded at Cardoso Island of the southern coast of the State of São Paulo, southeastern Brazil (Pessenda at al., 2012).

Although the stratigraphic sequence studied is compatible with the trends of global sea-level changes, the position of the sedimentary deposits that represent the deltaic system are positioned at least 20 m above the elevation expected for the MIS3 stage. A tectonic uplift in the study area during the Quaternary can be invoked to explain the difference in the paleo sea-levels, inasmuch as the late Pleistocene marine terrace deposits in northeastern Brazil suggests that the littoral zone may have been uplifted by at least 10–12 m since 120 ky B.P. (Barreto et al., 2002). In addition, regressive–transgressive events recorded along the Brazilian coast likely responded to a combination of eustatic sea-level fluctuations and local factors such as tectonic activity (Rossetti et al., 2013). These changes may contribute to accumulation of old marine deposits close to the modern coastline (Rossetti et al., 2011), as recorded in core Li01 by marine/brackish organic matter, marine shells and mangrove pollen in the deltaic system (Fig. 3).

The estuary containing mangroves recorded in core Li24 was formed during the high relative sea-level of the Holocene. These environments were likely formed during the early and middle Holocene as a response of a eustatic sea-level rise that resulted in significant changes in the coastal geomorphology (Fig. 6). During the early Holocene, arboreal and herbaceous vegetation dominated the coastal plain, and the equilibrium between the relative sea-level and fluvial sediment supply created conditions suitable for the development of an estuarine system with fluvial and tidal channels and of tidal flats colonized by mangroves (Fig. 6).

The upward succession composed of the transition from the estuarine complex with mangroves into the coastal plain colonized by marshes in core Li24 suggests a decrease in marine influence and forms the regressive part of the cycle after post glacial sea-level rise. Thus, the upper sequence of core Li24 (A5 and A3) should have accumulated following a relative sea-level fall or a high fluvial sediment supply during the middle and late Holocene. Considering the increase in sand input evidenced by fluvial channels, the fluvial sediment was reworked by wave and/or elevated water levels (e.g. storm surges) (Hesp et al., 2005). This process created the sandy ridges with replacement of mangroves by the groups of trees/shrubs and herbaceous vegetation consistent with a marine regression.

7. Sea-level changes and fluvial sediment supply

According to Posamentier et al. (1992), the term "regression" describes a retreat of the sea and a concomitant seaward expansion of the land. Regression can occur in two specific ways: (1) if sediment flux delivered to the shoreline exceeds the amount of space added for sediment to fill; and (2) if there is a relative sea-level fall. In either case, the shoreline migrates seaward. In situation 1, sufficient sediment is entering into the coastal system so as to overwhelm the amount of space available. This situation can occur during stillstands or rises of relative sea-level (which is a function of sea surface movement, i.e., eustasy and sea floor movement, the latter due to tectonics, thermal cooling, loading by sediments or by water, and sediment compaction) and is referred to as a "normal" regression. However, in certain cases, regression may not occur despite high volumes of sediment flux if the dispersive energy of the littoral environmental (i.e., waves or tidal currents) is high. Under these circumstances, supplied sediment is distributed over a wide area commonly beyond the immediate area, thus preventing progradation of the shoreline.

When no sediment is delivered to the shoreline during a relative sea-level fall, the regression is said to be forced because a seaward shift of the shoreline must occur, even if the volume of sediment supplied is zero. This situation is in marked contrast to "normal" regression, which occurs in response to the balance between variations of sediment flux and new space added (Posamentier et al., 1992).

In the first situation, regression can occur even under conditions of eustatic sea-level rise, because the rate of sediment flux is greater than the rate of increase of accommodation. Consequently, in areas of relatively high sediment flux, such as deltas, regression will continue longer following a sea-level rise, unlike in areas of relatively low sediment flux. Thus, despite the eustatic sea-level rise recorded on the southeastern Brazilian littoral during the early and middle Holocene that was followed by a relative sea-level fall (e.g., Suguio et al., 1985; Angulo et al., 2006), the high sediment flux of the Doce and Barra Seca River may have contributed to the regressive sequence evident since the middle Holocene.

8. Conclusion

Between ~47,500 and ~29,400 cal yr B.P., a deltaic system was developed in response mainly to the eustatic sea-level fall of the MIS3 stage. Although the studied stratigraphic succession is compatible with the trend of global sea-level fall, the previous sea-level stand, as suggested by the topographic position of these deltaic deposits, is above the one expected during the MIS3 stage. Tectonic uplift likely occurred during the late Quaternary and raised these deposits. The sedimentary sequence that accumulated during the LGM and the late Pleistocene/Holocene transition was eroded as a consequence of the rapid post glacial sea-level rise. The eustatic sea-level rise caused a marine incursion with invasion of coastal embayments and broad valleys, and it favored the evolution of an estuary with wide tidal mud flats occupied by mangroves between ~7400 and ~5100 cal yr B.P. During the late Holocene, abundant river sand supply and/or the relative sea-level fall led to seaward and downward translation of the shoreline during normal/forced regression, producing progradational deposits with shrinkage of mangroves and expansion of marshes colonized by herbaceous vegetation.

Our study of the deltaic plain of Doce River provides a case study that illustrates a stratigraphic sequence with development of deltaic systems and estuaries produced by the interplay of eustatic sea-level fluctuations and local factors such as sediment supply and tectonic activity.

Acknowledgments

We thank the members of the Laboratory of Coastal Dynamics (LADIC-UFPA), Center for Nuclear Energy in Agriculture (CENA-USP), and Vale Natural Reserve, Linhares, ES, for their support. This study was financed by the FAPESP (03615-5/2007 and 00995-7/2011). The authors also thank Franklin N. Santos for identifying the shells.

References

Absy, M.L., 1975. Polen e esporos do Quaternário de Santos (Brasil). Hoehnea 5, 1–26.
Angulo, R.J., Lessa, G.C., Souza, M.C., 2006. A critical review of mid- to late-Holocene sea-level fluctuations on the eastern Brazilian coastline. Quat. Sci. Rev. 25, 486–506.
Arai, M., 2006. A grande elevação eustática do Mioceno e sua influência na origem do Grupo Barreiras. Geologia USP Série Científica 6 (2), 1–6.
Asmus, H.E., Gomes, J.B., Pereira, A.C.B., 1971. Integração geológica regional da bacia do Espírito Santo. Anais do XXV Congresso Brasileiro de Geologia (SBG). São Paulo, SP, Brasil, pp. 235–254.
Bard, E., Hamelin, B., Fairbanks, R.G., 1990. U–Th ages obtained by mass spectrometry in corals from Barbados: sea level during the past 130,000 years. Nature 346, 456–458.
Bard, E., Hamelin, B., Arnold, M., Montaggioni, L., Cabioch, G., Faure, G., Rougerie, F., 1996. Deglacial sea-level record from Tahiti corals and the timing of global meltwater discharge. Lett. Nat. 382, 241–244.
Bard, E., Hamelin, B., Delanghe-Sabatier, D., 2010. Deglacial meltwater pulse 1B and Younger Dryas sea levels revisited with boreholes at Tahiti. Science 327, 1235–1237.
Barreto, A.M.F., Bezerra, F.H.R., Suguio, K., Tatumi, S.H., Yee, M., Paiva, R.P., Munita, C.S., 2002. Late Pleistocene marine terrace deposits in northeastern Brazil: sea level change and tectonic implications. Palaeogeogr. Palaeoclimatol. Palaeoecol. 179, 57–69.
Bassinot, F., Labeyrie, L., Vincent, E., Quidelleur, X., Lancelot, N.J., Lancelot, Y., 1994. The astronomical theory of climate and the age of the Brunhes–Matuyama magnetic reversal. Earth Planet. Sci. Lett. 126, 91–108.
Behling, H., 1996. First report on new evidence for the occurrence of Podocarpus and possible human presence at the mouth of the Amazon during the Late-glacial. Veg. Hist. Archaeobotany 5, 241–246.
Behling, H., 2001. Late Quaternary environmental changes in the Lagoa da Curuca region (eastern Amazonia) and evidence of Podocarpus in the Amazon lowland. Veg. Hist. Archaeobotany 10, 175–183.
Behling, H., Berrio, J.C., Hooghiemstra, H., 1999. Late quaternary pollen records from the middle Caquetá river basin in central Colombian Amazon. Palaeogeogr. Palaeoclimatol. Palaeoecol. 145, 193–213.
Berné, S., Jouet, G., Bassetti, M.A., Dennielou, B., Taviani, M., 2007. Late glacial to preboreal sea-level rise recorded by the Rhône deltaic system (NW Mediterranean). Mar. Geol. 245, 65–88.
Bruguière, J.G., 1789. Encyclopédie Méthodique. Histoire naturelle des Vers. Panckoucke, Paris, pp. i–xviii, 1–757.
Bruun, P., 1962. Sea level rise as a cause of shore erosion. Am. Soc. Civ. Eng. Proc J. Waterw. Harb. Div. 88, 117–130.
Burbridge, R.E., Mayle, F.E., Killeen, T.J., 2004. Fifty-thousand-year vegetation and climate history of Noel Kempff Mercado National Park, Bolivian Amazon. Quat. Res. 61, 215–230.
Bush, M.B., De Oliveira, P.E., Colinvaux, P.A., Miller, M.C., Moreno, J.E., 2004. Amazonian paleoecological histories: one hill, three watersheds. Palaeogeogr. Palaeoclimatol. Palaeoecol. 214, 359–393.
Cahoon, D.R., Hensel, P.F., Spencer, T., Reed, D.J., McKee, K.L., Saintilan, N., 2006. Coastal wetland vulnerability to relative sea-level rise: wetland elevation trends and process controls. In: Verhoeven, J.T.A., Beltman, B., Bobbing, R., Whigham, D.F. (Eds.), Wetlands and Natural Resource Management. Springer-Verlag, Berlin, pp. 271–292.
Carvalho, L.M.V., Jones, C., Liebmann, B., 2004. The South Atlantic Convergence Zone: intensity, form, persistence, and relationships with intraseasonal to interannual activity and extreme rainfall. J. Clim. 17, 88–108.
Chappell, J., Shackleton, N.J., 1986. Oxygen isotopes and sea level. Nature 324, 137–140.
Chappell, J., Woodroffe, C.D., 1994. Macrotidal estuaries. In: Carter, R.W.G., Woodroffe, C.D. (Eds.), Coastal Evolution: Late Quaternary Shoreline Morphodynamics. Cambridge Univ. Press, Cambridge, pp. 187–218.
Clark, J., McCabe, A.M., Schnabel, C., Clark, P.U., Freeman, S., Maden, C., Xu, S., 2009. ^{10}Be Chronology of the Last Deglaciation of County Donegal, Northwestern Ireland. Boreas 38, 111–118.
Cohen, M.C.L., Behling, H., Lara, R.J., 2005a. Amazonian mangrove dynamics during the last millennium: the relative sea-level and the little Ice Age. Rev. Palaeobot. Palynol. 136, 93–108.
Cohen, M.C.L., Souza Filho, P.W., Lara, R.L., Behling, H., Angulo, R., 2005b. A model of Holocene mangrove development and relative sea-level changes on the Bragança Peninsula (northern Brazil). Wetl. Ecol. Manag. 13, 433–443.
Colinvaux, P.A., De Oliveira, P.E., Moreno, J.E., Miller, M.C., Bush, M.B., 1996. A long pollen record from lowland Amazonia: forest and cooling in glacial times. Science 274, 85–87.
Colinvaux, P.A., De Oliveira, P.E., Patiño, J.E.M., 1999. Amazon Pollen Manual and Atlas – Manual e Atlas Palinológico da Amazônia. Hardwood Academic, Amsterdam.
Colinvaux, P.A., De Oliveira, P.E., Bush, M.B., 2000. Amazonian and neotropical plant communities on glacial time-scales: the failure of the aridity and refuge hypotheses. Quat. Sci. Rev. 19, 141–169.
Cutler, K.B., Edwards, R.L., Taylor, F.W., Cheng, H., Adkins, J., Gallup, C.D., Cutler, P.M., Burr, G.S., Bloom, A.L., 2003. Rapid sea-level fall and deep ocean temperature change since the last interglacial period. Earth Planet. Sci. Lett. 206, 253–271.
D'Alpaos, A., Lanzoni, S., Marani, M., Rinaldo, A., 2007. Landscape evolution in tidal embayments: modeling the interplay of erosion, sedimentation, and vegetation dynamics. J. Geophys. Res. Earth Surf. 112, 1–17.
Da Costa, E.M., 1778. Historia Naturalis Testaceorum Britanniae. White, Elmsley & Robson, London: Millan, p. 254. 17pls.
Dall, W.H., 1881. Reports on the results of dredging, under the supervision of Alexander Agassiz, in the Gulf of Mexico and in the Caribbean Sea (1877–78), by the United States Coast Survey Steamer "Blake", Lieutenant-Commander C.D. Sigsbee, U.S.N., and Commander J.R. Bartlett, U.S.N., commanding. XV. Preliminary report on the Mollusca. Bull. Mus. Comp. Zool. Harv. Coll. 9 (2), 33–144.
Dall, W.H., 1890. Scientific results of explorations by the U. S. Fish Commission Steamer Albatross. No. VII.—preliminary report on the collection of Mollusca and Brachiopoda obtained in 1887–'88. Proceedings of the United States National Museum, 12 (773), pp. 219–362 (pls. 5–14).
Dalrymple, R.W., Knight, R.J., Zaitlin, B.A., Middleton, G.V., 1990. Dynamics and facies model of a macrotidal sand-bar complex, Cobequid Bay-Salmon River estuary (Bay of Fundy). Sedimentology 37, 577–612.
Dalrymple, W.R., Zaitlin, B.A., Boyd, R., 1992. Estuarine facies models: conceptual basis and stratigraphic implications. J. Sediment. Petrol. 62 (6), 1130–1146.
Dominguez, J.M.L., 2009. The coastal zone of Brazil. In: Dillenburg, S.R., Hesp, P.A. (Eds.), Geology and Geomorphology of Holocene Coastal Barriers of Brazil. Springer-Verlag, Berlin, pp. 17–51.
Dominguez, J.M.L., Bittencourt, A.C.S.P., Martin, L., 1992. Controls on Quaternary coastal evolution of the east-northeastern coast of Brazil: roles of sea-level history, trade winds and climate. Sediment. Geol. 80, 213–232.
Duclos, P.L., 1840. Histoire Naturelle Générale et de Tous les Particulière Genres de Coquilles Marines univalves vivant l'etat et um Fossile, Monografias par Publiee, Columbella Gênero. Didot, Paris 1 (13 pls).
Evin, J., Marechal, J., Pachiaudi, C., 1980. Conditions involved in dating terrestrial shells. Radiocarbon 22, 545–555.
Faegri, K., Iversen, J., 1989. Textbook of Pollen Analysis, 4th. John Wiley and Sons, Chichester.
Fairbanks, R.G., 1989. A 17,000-year glacio-eustatic sea level record: influence of glacial melting dates on the Younger Dryas event and deep-ocean circulation. Nature 342, 637–642.
França, M.C., Cohen, M.C.L., Pessenda, L.C.R., Rossetti, D.F., Lorente, F.L., Buso Jr., A.A., Guimarães, J.T.F., Friaes, Y.S., 2013. Mangrove dynamics in response to sea-level changes on Holocene terraces of the Doce River, southeastern Brazil. Catena 110, 59–69.
French, J.R., Stoddart, D.R., 1992. Hydrodynamics of saltmarsh creek systems: implications for marsh morphological development and material exchange. Earth Surf. Process. Landf. 17, 235–252.
Furukawa, K., Wolanski, E., 1996. Sedimentation in mangrove forests. Mangrove Salt Marshes 1, 3–10.
Goodfriend, G.A., 1987. Radiocarbon age anomalies in shell carbonate of land snails from semi-arid areas. Radiocarbon 29, 159–167.
Goodfriend, G.A., Stipp, J.J., 1983. Limestone and the problem of radiocarbon dating of land-snail shell carbonate. Geology 11, 575–577.
Gray, J.E., 1825. A list and descriptions of some species of shells not taken notice of by Lamarck. Ann. Philos. (new series) 9, 134–140.
Grimm, E.C., 1987. Coniss: a Fortran 77 program for stratigraphically constrained cluster analysis by the method of the incremental sum of square. Comput. Geoscie. 13, 13–35.
Haberle, S.G., Maslin, M.A., 1999. Late Quaternary vegetation and climate change in the Amazon Basin based on a 50,000 year pollen record from the Amazon Fan, ODP Site 932. Quat. Res. 51, 27–38.
Harper, C.W., 1984. Improved methods of facies sequence analysis, In: Walker, R.G. (Ed.), Facies Models, second ed. Geological Association of Canada, Ontario, Canada, pp. 11–13.
Hesp, P.A., Dillenburg, S.R., Barboza, E.G., Tomazelli, L.J., Ayup-Zouain, R.N., Esteves, L.S., Gruber, N.L.S., Toldo Jr., E.E., Tabajara, L.L.C.D.A., Clerot, L.C.P., 2005. Beach ridges, foredunes or transgressive dunefields? Definitions and an examination of the Torres to Tramandaí barrier system, Southern Brazil. An. Acad. Bras. Cienc. 77, 493–508.
Imbrie, J., Hays, J.D., Martinson, D.G., McIntyre, A., Mix, A.C., Morley, J.J., Pisias, N.G., Prell, W.L., Shackleton, N.J., 1984. The orbital theory of Pleistocene climate: support from a revised chronology of the marine δ O18 record. In: Berger, A., Imbrie, J., Hays, J., Kukla, G., Saltzman, B. (Eds.), Milankovitch and Climate. Reidel Publishing Company, Dordrecht, pp. 269–305.
Kirwan, M.L., Murray, A.B., 2007. A coupled geomorphic and ecological model of tidal marsh evolution. Proc. Natl. Acad. Sci. 104, 6118–6122.
Labeyrie, L.D., Duplessy, J.C., Blanc, P.L., 1989. Variations in mode of formation and temperature of oceanic deep waters over the past 125,000 years. Nature 327, 477–482.
Lamb, A.L., Wilson, G.P., Leng, M.J., 2006. A review of coastal palaeoclimate and relative sea-level reconstructions using δ13C and C/N ratios in organic material. Earth Sci. Rev. 75, 29–57.
Lambeck, K., 1997. Sea-level change along the French Atlantic and channel coasts since the time of the Last Glacial Maximum. Palaeogeogr. Palaeoclimatol. Palaeoecol. 129, 1–22.

Lambeck, K., Bard, E., 2000. Sea-level change along the French Mediterranean coast for the past 30,000 years. Earth Planet. Sci. Lett. 175, 203–222.
Lambeck, K., Chappell, J., 2001. Sea level change through the Last Glacial cycle. Science 292, 679–686.
Lambeck, K., Yokoyama, Y., Purcell, T., 2002. Into and out of the Last Glacial Maximum: sea-level change during oxygen isotope stages 3 and 2. Quat. Sci. Rev. 21, 343–360.
Lambeck, K., Antonioli, F., Purcell, A., Silenzi, S., 2004a. Sea-level change along the Italian coast for the past 10,000 yr. Quat. Sci. Rev. 23, 1567–1598.
Lambeck, K., Anzidei, M., Antonioli, F., Benini, A., Esposito, A., 2004b. Sea level in Roman time in the Central Mediterranean and implications for recent change. Earth Planet. Sci. Lett. 224, 463–575.
Ledru, M.P., Cordeiro, R.C., Dominguez, J.M.L., Martin, L., Mourguiart, P., Sifeddine, A., Turcq, B., 2001. Late-Glacial cooling in Amazonia inferred from pollen at Lagoa do Caçó, Northern Brazil. Quat. Res. 55, 47–56.
Link, D.H.F., 1807. Beschreibung der Naturalien–Sammlung der Universität zu Rostock. Alders Erben, Rostock (166 pp.).
Markgraf, V., D'Antoni, H.L., 1978. Pollen Flora of Argentina. University of Arizona Press, Tucson.
Martin, L., Suguio, K., 1992. Variation of coastal dynamics during the last 7000 years recorded in beach-ridge plains associated with river mouths: example from the central Brazilian coast. Palaeogeogr. Palaeoclimatol. Palaeoecol. 99, 119–140.
Martin, L., Dominguez, J.M.L., Bittencourt, A.C.S.P., 1998. Climatic control on coastal erosion during a sea-level fall episode. An. Acad. Bras. Cienc. 70, 249–266.
Martin, L., Dominguez, J.M.L., Bittencourt, A.C.S.P., 2003. Fluctuating Holocene sea levels is eastern and southeastern Brazil: evidence from a multiple fossil and geometric indicators. J. Coast. Res. 19, 101–124.
Mayle, F.E., Burbridge, R., Killeen, T.J., 2000. Millennial-scale dynamics of southern Amazonian rain forests. Science 290, 2291–2294.
McKee, K.L., Cahoon, D.R., Feller, I.C., 2007. Caribbean mangroves adjust to rising sea level through biotic controls on change in soil elevation. Glob. Ecol. Biogeogr. 16, 545–556.
Meyers, P.A., 1994. Preservation of source identification of sedimentary organic matter during and after deposition. Chem. Geol. 114, 289–302.
Meyers, P.A., 2003. Applications of organic geochemistry to paleolimnological reconstructions: a summary of examples from the Laurentian Great Lakes. Org. Geochem. 34, 261–289.
Miall, A.D., 1978. Facies types and vertical profile models in braided river deposits: a summary. In: Miall, A.D. (Ed.), Fluvial Sedimentology. Canadian Society of Petroleum Geologists, Calgary, pp. 597–604.
Orbigny, A.D., 1841. Paléontologie française. Description zoologique et géologique de tous les animaux mollusques et rayonnés fossiles de France. Terrains Crétacés. Céphalopodes. Paris, Masson, Part II, Tome 1 121–430.
Orbigny, A.D., 1846. Mollusques. In: Bertrand, P. (Ed.), Voyage dans l'Amérique Meridionale (le Bresil) execute pendant les annes 1829–1833 (Paris, v. 5, pt. 3, 758 pp., 85 pls).
Otvos, E.G., 2000. Beach ridges—definitions and significance. Geomorphology 32, 83–108.
Peixoto, A.L., Gentry, A., 1990. Diversidade e composição florística da mata de tabuleiros na Reserva Florestal de Linhares (Espírito Santo, Brasil). Rev. Bras. Bot. 13 (1), 19–25.
Peltier, W.R., Fairbanks, R.G., 2006. Global glacial ice volume and Last Glacial Maximum duration from an extended Barbados sea level record. Quat. Sci. Rev. 25, 3322–3337.
Pessenda, L.C.R., Ribeiro, A.S., Gouveia, S.E.M., Aravena, R., Boulet, R., Bendassoli, J.A., 2004. Vegetation dynamics during the late Pleistocene in the Barreirinhas region, Maranhão State, northeastern Brazil, based on carbon isotopes in soil organic matter. Quat. Res. 62, 183–193.
Pessenda, L.C.R., Vidotto, E., De Oliveira, P.E., Cohen, M.C.L., Buso Jr., A.A., Rossetti, D.F., Ricardi-Branco, F., Bendassolli, J.A., 2012. Late Quaternary vegetation and coastal environmental changes at Ilha do Cardoso mangrove, southeastern Brazil. Palaeogeogr. Palaeoclimatol. Palaeoecol. 363–364, 57–68.
Philippi, R.A., 1841. Zoologische Bemerkungen. Archiv für Naturgeschichte, Berlin, 7. 1 42–59 pl. 5.
Pigati, J.S., McGeehin, J.P., Muhs, D.R., Bettis, E.A., 2013. Radiocarbon dating late Quaternary loess deposits using small terrestrial gastropod shells. Quat. Sci. Rev. 76, 114–128.
Posamentier, H.W., Allen, G.P., James, D.P., Tesson, M., 1992. Forced regressions in a sequence stratigraphic framework: concepts, examples, and exploration significance. Am. Assoc. Pet. Geol. Bull. 76, 1687–1709.
Rabineau, M., Berné, S., Aslanian, D., Olivet, J.L., Joseph, P., Guillocheau, F., Bourillet, J.F., Ledrezen, E., Granjeon, D., 2006. Paleo sea levels reconsidered from direct observation of paleoshoreline position during Glacial Maxima (for the last 500,000 yr). Earth Planet. Sci. Lett. 252, 119–137.
Reimer, P.J., Baillie, M.G.L., Bard, E., Bayliss, A., Beck, J.W., Blackwell, P.G., Bronk Ramsey, C., Buck, C.E., Burr, G.S., Edwards, R.L., Friedrich, M., Grootes, P.M., Guilderson, T.P., Hajdas, I., Heaton, T.J., Hogg, A.G., Hughen, K.A., Kaiser, K.F., Kromer, B., Mccormac, F.G., Manning, S.W., Reimer, R.W., Richards, D.A., Southon, J.R., Talamo, S., Turney, C.S.M., Van der Plicht, J., Weyhenmeyer, C.E., 2009. IntCal09 and Marine09 radiocarbon age calibration curves, 0–50,000 years cal BP. Radiocarbon 51, 1111–1150.
Reis, A.T., Maia, R.M.C., Silva, C.G., Rabineau, M., Guerra, J.V., Gorini, C., Ayres, A., Arantes-Oliveira, R., Benabdellouahed, M., Simões, I.C.V.P., Tardin, R., 2013. Origin of step-like and lobate seafloor features along the continental shelf off Rio de Janeiro State. Santos Basin-Brazil. Geomorphology V. Special, 1–18.
Rohling, E.J., Fenton, M., Jorissen, F.J., Bertrand, P., Ganssen, G., Caulet, J.P., 1998. Magnitudes of sea level lowstands of past 500,000 years. Nature 394, 162–165.
Rossetti, D.F., Bezerra, F.H., Góes, A.M., Valeriano, M.M., Andrades Filho, C.O., Mittani, J.C.R., Tatumi, S.H., Brito-Neves, B.B., 2011. Late Quaternary sedimentation in the Paraíba Basin, Northeastern Brazil: landform, sea level and tectonics in Eastern South America passive margin. Palaeogeogr. Palaeoclimatol. Palaeoecol. 300, 191–204.
Rossetti, D.F., Bezerra, F.H., Dominguez, J.M.L., 2013. Late Oligocene-Miocene transgressions along the equatorial and eastern margins of Brazil. Earth Sci. Rev. 123, 87–112.
Roubik, D.W., Moreno, J.E., 1991. Pollen and Spores of Barro Colorado Island, vol. 36. Missouri Botanical Garden, St. Louis.
Rubin, M., Likins, R.C., Berry, E.G., 1963. On the validity of radiocarbon dates from snail shells. J. Geol. 71, 84–89.
Ruddiman, W.F., 2008. The challenge of modeling interglacial CO_2 and CH_4 trends. Quat. Sci. Rev. 27, 445–448.
Salgado-Labouriau, M.L., 1973. Contribuição à palinologia dos cerrados. Academia Brasileira de Ciências, Rio de Janeiro (273 pp.).
Say, T., 1822. An account of some of the marine shells of the United States. J. Acad. Nat Sci. Phila. 2, 228.
Schidlowski, M., Hayes, J.M., Kaplan, I.R., 1983. Isotopic inferences of ancient biochemistries: carbon, sulphur, hydrogen and nitrogen. In: Scholf, J.W. (Ed.), Earth's Earliest Biosphere, Its Origin and Evolution. Princeton University Press, Princeton, pp. 149–186.
Schwartz, M.L., 1965. Laboratory study of sea-level rise as a cause of shore erosion. J. Geol. 73, 528–534.
Schwartz, M.L., 1968. The scale of shore erosion. J. Geol. 76, 508–517.
Shackleton, N.J., 2000. The 100,000-year Ice-Age cycle identified and found to lag temperature, carbon dioxide, and orbital eccentricity. Science 289, 1897–1902.
Siddall, M., Almogi-Labin, R.E.J.A., Hemleben, C., Meischner, D., Schmelzer, I., Smeed, D.A., 2003. Sea-level fluctuations during the last glacial cycle. Nature 423, 853–858.
Skene, K.I., Piper, D.J.W., Aksu, A.E., Syvitski, J.P.M., 1998. Evaluation of the global oxygen isotope curve as a proxy for Quaternary sea level by modeling of delta progradation. J. Sediment. Res. 68, 1077–1092.
Stute, M., Clark, J.F., Schlosser, P., Broecker, W.S., 1995. A 30,000 yr continental paleotemperature record derived from noble gases dissolved in groundwater from the San Juan basin, New Mexico. Quat. Res. 43, 209–220.
Suguio, K., Martin, L., Bittencourt, A.C.S.P., Dominguez, J.M.L., Flexor, J.M., Azevedo, A.E.G., 1985. Flutuações do Nível do Mar durante o Quaternário Superior ao longo do Litoral Brasileiro e suas Implicações na Sedimentação Costeira. Rev. Bras. Geosci. 15, 273–286.
Suter, J.R., 1994. Deltaic coasts. In: Carter, R.W.G., Woodroffe, C.D. (Eds.), Coastal Evolution: Late Quaternary Shoreline Morphodynamics. Cambridge University Press, Cambridge, pp. 87–120.
Swift, D.J.P., 1975. Barrier island genesis: evidence from the central Atlantic Shelf, eastern USA. Sediment. Geol. 14, 1–43.
Toscano, M.A., Lundberg, J., 1999. Submerged Late Pleistocene reefs on the tectonically stable SE Florida margin: high precision geochronology, stratigraphy, resolution of Substage 5a sea-level elevation, and orbital forcing. Quat. Sci. Rev. 18, 753–767.
Urrego, D.H., Silman, M.R., Bush, M.B., 2005. The Last Glacial Maximum: stability and change in a western Amazonian cloud forest. J. Quat. Sci. 20 (7–8), 693–701.
van Meerbeeck, C.J., Renssen, H., Roche, D.M., 2009. How did Marine Isotope Stage 3 and Last Glacial Maximum climates differ? Perspectives from equilibrium simulations. Climate of the Past Discussions 4, 1115–1158.
Waelbroeck, C., Labeyrie, L.D., Michel, E., Duplessy, J.-C., McManus, J., Lambeck, K., Balbon, E., Labracherie, M., 2002. Sea level and deep water changes derived from benthic Foraminifera isotopic record. Quat. Sci. Rev. 21, 295–305.
Walker, R.G., 1992. Facies, facies models and modern stratigraphic concepts. In: Walker, R.G., James, N.P. (Eds.), Facies Models—Response to Sea Level Change. Geological Association of Canada, Ontario, pp. 1–14.
Wentworth, C.K., 1922. A scale of grade and class terms for clastic sediments. J. Geol. 30, 377–392.
Whitney, B.S., Mayle, F.E., Punyasena, S.W., Fitzpatrick, K.A., Burn, M.J., Guillen, R., Chavez, E., Mann, D., Pennington, R.T., Metcalfe, S.E., 2011. A 45 kyr paleoclimate record from the lowland interior of tropical South America. Palaeogeogr. Palaeoclimatol. Palaeoecol. 307, 177–192.
Woodroffe, C.D., 1995. Response of tide-dominated mangrove shorelines in northern Australia to anticipated sea-level rise. Earth Surf. Process. Landf. 20, 65–85.
Woodroffe, C.D., 2002. Coasts: Form, Process and Evolution. Cambridge University Press, Cambridge.
Woodroffe, C.D., Chappell, J.M.A., Thom, B.G., Wallensky, E., 1989. Depositional model of a macrotidal estuary and flood plain, South Alligator River, Northern Australia. Sedimentology 36, 737–756.